ANL/CP--73475

DE91 015110

RADIATION-INDUCED AMORPHIZATION OF INTERMETALLIC COMPOUNDS. A MOLECULAR-DYNAMICS STUDY OF CuTi AND Cu_4Ti_3 *

N. Q. LAM[1], M. J. SABOCHICK[2] and P. R. OKAMOTO[1]

[1] Materials Science Division, Argonne National Laboratory, Argonne, IL 60439

[2] Department of Engineering Physics, Air Force Institute of Technology, Wright-Patterson AFB, OH 45433

June 1991

- Presented at the IEA Workshop on The Use of Molecular Dynamics in Modeling Radiation Effects and Other Nonequilibrium Phenomena, May 6-8, 1991, La Jolla, CA.
- To be published in *Radiation Effects and Defects in Solids*

*Work supported by the U.S. Department of Energy, BES-Materials Sciences, under Contract W-31-109-Eng-38.

RADIATION-INDUCED AMORPHIZATION OF INTERMETALLIC COMPOUNDS. A MOLECULAR-DYNAMICS STUDY OF CuTi AND Cu_4Ti_3 *

N. Q. LAM[1], M. J. SABOCHICK[2] and P. R. OKAMOTO[1]

[1] Materials Science Division, Argonne National Laboratory, Argonne, IL 60439
[2] Department of Engineering Physics, Air Force Institute of Technology, Wright-Patterson AFB, OH 45433

ABSTRACT

In the present paper, important results of our recent computer simulation of radiation-induced amorphization in the ordered compounds CuTi and Cu_4Ti_3 are summarized. The energetic, structural, thermodynamic and mechanical responses of these intermetallics during chemical disordering, point-defect production and heating were simulated, using molecular dynamics and embedded-atom potentials. From the atomistic details obtained, the critical role of radiation-induced structural disorder in driving the crystalline-to-amorphous phase transformation is discussed.

---

* Work supported by the U.S. Department of Energy, BES-Materials Sciences, under Contract W-31-109-Eng-38.

INTRODUCTION

One of the nonequilibrium phenomena that occurs in many alloy systems during irradiation is the crystalline-to-amorphous (c-a) phase transition, or the so-called radiation-induced amorphization. The amorphous phase was observed in ion-bombarded alloys, ion-mixed thin films, ion-implanted layers, and regions irradiated by energetic electrons inside a high-voltage electron microscope. Due to its simplicity, however, electron irradiation-induced amorphization has been investigated most systematically over the last decade (see, e.g., [1,2] and references therein). To date, most of those alloys that become amorphous under electron irradiation are high-temperature intermetallic compounds which are composed of early transition or refractory elements with unpaired d-electrons (e.g., Ti, Zr, V, Mo) and the late transition or noble metals having nearly filled d-shells and significantly smaller size (>15%) than that of the early transition metal group (e.g., Fe, Co, Ni, Cu).

Amorphization induced by electron irradiation represents the simplest case of c-a transitions to study, both experimentally and theoretically, because only Frenkel pairs are involved; concepts like thermal spike, local melting or quenching can be safely excluded. There is, however, a drawback in the experimental investigation, since it is difficult to determine which mechanism, chemical disordering or point-defect creation, is dominant in inducing amorphization. This arises because of the fact that the incident electrons produce lattice defects which, in turn, result in chemical disorder and volume expansion, both of which are always observed to occur prior to the c-a transition. Due to the lack of such atomistic details about the evolving physical properties of alloy systems under irradiation, many experimental measurements could not be interpreted unambiguously.

To provide more information for the interpretation of experiments, a number of molecular-dynamics studies have been carried out in recent years [3-7]. In computer simulations, one can easily induce chemical disorder or vary the system volume without introducing of point defects, and thus the individual effects of these mechanisms can be determined. Unfortunately, due to the lack of appropriate interatomic potentials for alloys, most of these simulations have so far been performed on monatomic solids [3-5]. Most recently, we have begun a series of molecular-dynamics simulations of radiation-induced amorphization [8-10] and point-defect behavior [11,12] in several intermetallics, using interatomic potentials developed with the embedded-atom method [13,14]. The present paper summarizes a number of simulation results that was obtained for two intermetallic compounds of the Cu-Ti alloy system, CuTi and Cu_4Ti_3. It should be pointed out that among alloy systems investigated experimentally, the intermetallic compounds of the Cu-Ti system have been studied most systematically [1]. The results of our computer simulations indicate that the conclusion of previous investigators concerning the role of chemical disorder in inducing amorphization of these compounds needs to be re-examined.

MODEL AND COMPUTATIONAL PROCEDURE

The crystal structures of the compounds studied in the present work are shown in Figure 1. The model lattice that represents the ordered CuTi compound has a B11 structure, with a stacking of two body-centered tetragonal sublattices and bilayer arrangement of Cu and Ti atoms. The structure of Cu_4Ti_3 is more complicated; it is a Frank-Kasper-type structure, consisting of seven stacked body-centered tetragonal sublattices. The interactions between the atoms in the model system were governed by appropriate potentials, which were developed with the approach of Oh and Johnson [14], based on the embedded-atom method [13]. Details

of the fitting procedure and functional form of the potentials are given elsewhere [8].

The primary simulation technique employed was a molecular-dynamics scheme modified from the code DYNAMO [15]. Briefly, for equilibration and property calculations, we used molecular dynamics, and for relaxing the system after the introduction of defects, we used molecular statics with the Fletcher-Powel minimization procedure [16]. The effect of chemical disordering was simulated by exchanging a random pair of Cu and Ti atoms; on the other hand, to simulate the production of a Frenkel pair, a randomly-selected atom was removed (creating a vacancy) and then re-inserted at a random position in the lattice (forming an interstitial). The simulation proceeded as follows.

A perfect lattice was first equilibrated for 5000 time steps (Δt), and then every $10\Delta t$, a random pair of antisite defects or a Frenkel pair was created. The system configuration was periodically saved during the defect production process, and subsequently equilibrated for additional $6000\Delta t$ in separate runs. The equilibrated systems were analyzed by comparing their potential energies, volumes, pair-correlation functions, atom projections, and elastic constants with those of the perfect lattice.

RESULTS AND DISCUSSION

Driving Force for Amorphization

Figure 2 shows the changes in physical properties and structure of the compound CuTi as a result of chemical disordering and Frenkel-pair production. Initially, as the number of atom exchanges or point defects increases, the system energy and volume rapidly increase. Most of Frenkel pairs created recombine resulting in the formation of antisite defects. As a consequence, the difference in the effects of the two types of defect production in the early stage is quite small.

When chemical disordering is produced via atom-pair exchanges, the system energy and volume expansion reach maximum values at a certain degree of disorder, and then slightly decrease when further atom exchanges are generated. This slight recovery in energy and volume was observed in all of our simulations of the chemical disordering effect, and could be attributed to local structural relaxations. The long-range order parameter decreases from 1 for the perfect lattice to ~0.13 at the point where the system energy and volume are maximum, and to ~0 when all the atoms in the system have been exchanged. While the effect of chemical disordering approaches saturation, the accumulation of point defects continues to boost the potential energy and system volume to levels above those of the quenched CuTi liquid, shown by the dashed lines. The lattice expansion tracks very closely the variations in total energy increase and, hence, provides a direct measure of the thermodynamic driving force for the phase transition.

The evolution of the compound microstructure is shown by the changes in the calculated pair-correlation functions and atomic projections onto the (001) planes (Figure 2). When all the Cu and Ti atoms have been exchanged, the system only becomes chemically disordered, but not amorphized, indicating that chemical disorder alone cannot lead to amorphization. When Frenkel pairs are created, however, the system becomes partially amorphized at a dose of ~0.5 dpa (displacements per atom), i.e., after ~50% of the atoms in the compound have been displaced, and completely amorphous at ~1.0 dpa. (Here, being different from previous definition based on pair-correlation functions [3-9], the critical dose for complete amorphization is defined as the point when the system becomes isotropic, i.e., when all the shear constants become equal.) The lattice softens considerably during the generation of Frenkel pairs, as indicated by the variations in the shear elastic constants, C_{44} and C', and their average values, $C_{avg} = (C_{44} + C')/2$ (Figure 2). The shear modulus C_{44} decreases rapidly with increasing dose and eventually

becomes equal to C' (which first decreases and then increases) when amorphization is completed. It is noted that small differences between C_{44} and C' still exist at a dose of ~0.5 dpa, even though calculated diffraction patterns exhibit a diffuse halo [10]. This may be attributed to the remains of tiny pockets of crystalline material inside the system.

Similar behavior was observed in Cu_4Ti_3, as shown in Figure 3. Although chemical disorder increases both the system energy and volume, the buildup of point defects beyond complete chemical disordering is necessary to trigger the crystalline-to-amorphous phase transition. Amorphization is completed at a critical dose of 0.6 dpa, at which point the two elastic moduli C_{44} and C' become equal.

The calculated critical doses for amorphization are in good agreement with experimental observations [17,18]. There is no measurements of the volume expansions in CuTi and Cu_4Ti_3 at the onset of amorphization. However, the simulation results appear consistent with that calculated previously for $NiZr_2$ [6], as well as with those obtained experimentally for other compounds, including Zr_3Al [19], NiAl [20], Nb_3Ge [21,22], and Mo_3Si [23].

Volume Dependence of Shear Elastic Constants

The average shear moduli C_{avg} and C' of CuTi and Cu_4Ti_3 are plotted in Figure 4, as a function of volume expansion brought about by heating, chemical disordering, and Frenkel-pair creation. Two observations can be made. First, the average shear modulus of the defective crystal drops significantly faster with volume expansion than that associated with heating. And second, when Frenkel pairs are generated, a ~50% reduction in the average shear modulus is observed at the onset of amorphization. The same behavior has been observed experimentally in the two compounds Zr_3Al [19] and FeTi [20].

The faster decrease of the average shear modulus C_{avg} of the structurally-disordered crystal with increasing volume expansion, relative to that of the perfect crystal during heating, can be interpreted in terms of additional contribution of the static component, $<\mu^2_{sta}>$, to the mean-square displacements of the atoms, $<\mu^2_T>$. In fact, according to Lindemann's vibrational catastrophe theory [24], melting of an ideal crystal is attributed to the onset of instability which arises when the atom mean-square displacements associated with thermal vibration of the lattice, $<\mu^2_{vib}>$, reaches a critical value $<\mu^2_{cri}>$, i.e.,

$$\text{when} \quad <\mu^2_{vib}> \rightarrow <\mu^2_{cri}> , \quad T \rightarrow T_m = \frac{Mk\theta^2}{9\hbar^2} <\mu^2_{cri}> \qquad (1)$$

where M is the atomic mass, k is the Boltzmann constant, and θ is the Debye temperature of the perfect crystal. In an irradiated crystal, however, we have

$$<\mu^2_T> = <\mu^2_{vib}> + <\mu^2_{sta}> . \qquad (2)$$

Generally, the static displacements $<\mu^2_{sta}>$ caused by the presence of defects are much larger than $<\mu^2_{vib}>$. As a result, irradiation can effectively increase $<\mu^2_T>$ toward the critical value $<\mu^2_{cri}>$ at low temperatures, and therefore the defective crystal becomes unstable at a temperature $T^d_{ins} << T_m$, defined as

$$T^{def}_{ins} = \frac{Mk\theta^2_{def}}{9\hbar^2} <\mu^2_{cri}> . \qquad (3)$$

Here, θ_{def}, the Debye temperature of the defective crystal, can be related to θ by

$$\theta_{def}^2 = \theta^2 \left[1 - \frac{<\mu_{sta}^2>}{<\mu_{cri}^2>} \right] \qquad (4)$$

Since the average shear modulus of many metals and intermetallic compounds scale directly with the square of the Debye temperature [25], and the volume expansion is proportional to the mean-square displacements of the atoms, equation (4) clearly shows that C_{avg} of the irradiated compound ($<\mu^2_T> \simeq <\mu^2_{sta}>$) decreases much faster with $\Delta V/V$ than that of an unirradiated compound subject to heating ($<\mu^2_T> = <\mu^2_{vib}>$).

Finally, during irradiation the c-a transition is triggered when the average shear modulus of the defective compound, C^d_{avg}, becomes equal to that of the amorphous phase, C^a_{avg}, [2], i.e., when

$$C^d_{avg} / C^c_{avg} = C^a_{avg} / C^c_{avg} = \theta_a^2 / \theta^2 \qquad (5)$$

with C^c_{avg} being the average shear modulus of the crystalline, unirradiated compound. Since the Debye temperatures of amorphous compounds, θ_a, are typically between 0.6θ and 0.8θ (see ,e.g., [2] and references therein), it is expected, from equation (5), that $C^d_{avg} / C^c_{avg} \simeq 0.5$ when amophization occurs.

SUMMARY

- Radiation-induced amorphization of CuTi and Cu_4Ti_3 was simulated, using molecular dynamics in conjunction with embedded-atom potentials. Changes in

the system energy, volume, pair-correlation functions, atom projection, and elastic constants were analyzed.

- Amorphization was found to occur in a two-step process: (i) introduction of chemical disorder via point-defect recombination, and (ii) stabilization and accumulation of point defects, leading to lattice instability. The buildup of point defects is a necessary factor for amorphization.

- The calculated damage doses required to render the compounds completely amorphous (~1.0 dpa for CuTi and 0.6 dpa for Cu_4Ti_3) and volume expansions after the c-a transition (~1.9% and 1.7%, respectively) are in general agreement with experimental observations.

- At the onset of amorphization, the average shear modulus decreases by a factor of ~2, in good accord with experiment.

REFERENCES

1. D.E. Luzzi and M. Meshii, *Res Mechanica* **21**, 207 (1987).
2. P.R. Okamoto and M. Meshii, *Science of Advanced Materials*, edited by H. Wiedersich and M.Meshii (American Society for Metals, Metals Park,OH, 1990), Chap. 2, pp. 33-98.
3. K. Maeda and S. Takeuchi, *Philos. Mag.* B **52**, 955 (1985).
4. H. Hsieh and S. Yip, *Phys. Rev. Lett.* **59**, 2760 (1987); *Phys. Rev.* B **39**, 7476 (1989).
5. Y. Limoge, A. Rahman, H.Hsieh, and S. Yip, *J. Non-Cryst. Solids* **99**, 75 (1988).
6. C. Massobrio, V. Pontikis, and G. Martin, *Phys. Rev. Lett.* **62**, 1142 (1989); Phys. Rev. B **41**, 10486 (1990).
7. M.J. Sabochick and N.Q. Lam, *Scr.Metall. Mater.* **24**, 565 (1990); *Mat. Res. Soc. Symp. Proc.* **157**, 265 (1990).
8. M.J. Sabochick and N.Q. Lam, *Phys. Rev.* B **43**, 5243 (1991).
9. M.J. Sabochick and N.Q. Lam, *Mat. Res. Soc. Symp. Proc.* (1991) in press.
10. R. Devanathan, N.Q. Lam, M.J. Sabochick, P. Okamoto, and M. Meshii, *Mat. Res. Soc. Symp. Proc.* (1991) in press.
11. J.R. Shoemaker, R.T. Lutton, D. Wesley, W.R. Wharton, M.L. Oehrli, M.S. Herte, M.J. Sabochick, and N.Q. Lam, *J. Mater. Res.* **6**, 473 (1991).
12. R.T. Lutton, M.J. Sabochick, and N.Q. Lam,*Mat. Res. Soc. Symp. Proc.* (1991) in press.
13. M.S. Daw and M.I. Baskes, *Phy. Rev.* B **29**, 6443 (1984).
14. D.J. Oh and R.A. Johnson, *J. Mater. Res.* **3**,471 (1988).
15. M.S. Daw, M.I. Baskes, and S.M. Foiles (private communication).
16. M.J. Sabochick and S. Yip, *J. Phys.* F **18**, 1689 (1988).

17. J. Koike, P.R. Okamoto, R.E. Rehn and M. Meshii, *J. Mater. Res.* 4, 1143 (1989).

18. D.E. Luzzi, H. Mori, H. Fujita, and M. Meshii, *Mat. Res. Soc. Symp. Proc.* **51**, 479 (1985).

19. P.R. Okamoto, L.E. Rehn, J. Pearson, R. Bhadra, and M. Grimsditch, *J. Less Common Met.* **140**, 291 (1988).

20. J. Koike, P.R. Okamoto, R.E. Rehn and M. Meshii, *Mat. Res. Soc. Symp. Proc.* **157**, 777 (1990).

21. J. Pfluger and O. Meyer, *Sol. State Comn.* **32**, 1143 (1979).

22. A.R. Sweedler. D.E. Cox, and S. Moehlecke, *J. Nucl. Mater.* **72**,, 50 (1978).

23. A.V. Mirmelshteyn, A. Ye Karlin, V. Ye Arkhipov, and V.I.Voronin, *Phys. Met. Metall.* **55**, 67 (1983).

24. A. Lindemann, *Z. Phys.* **11**, 609 (1910).

25. G. Grimvall and S. Sjodin, *Physica Scripta* **10**, 340 (1974).

FIGURE CAPTIONS

Fig. 1: Crystal structures of CuTi and Cu_4Ti_3.

Fig. 2: Changes in the potential energy, volume expansion and shear moduli as a function of the number of atom exchanges or Frenkel pairs per atom in CuTi. The values calculated for the quenched CuTi liquid are indicated by the horizontal dashed lines. Pair-correlation functions and atom projections are also shown for various doses: (A) perfect lattice, (B) after random exchange of all atoms, (C) after 0.434 dpa, (D) after 0.521 dpa, (E) after 0.694 dpa, and (F) quenched CuTi liquid from 4000 K. Note that C_{44}, C' and $C_{avg} = (C_{44} + C')/2$ are equal when the system becomes completely amorphized.

Fig. 3: Changes in the potential energy, volume expansion and shear moduli as a function of the number of atom exchanges or Frenkel pairs per atom in Cu_4Ti_3. The values calculated for the quenched Cu_4Ti_3 liquid are shown by the horizontal dashed lines. All the shear moduli C_{44}, C' and $C_{avg} = (C_{44} + C')/2$ become equal when the system is completely isotropic.

Fig. 4: Volume dependence of the average shear moduli C_{avg} and C' in CuTi and Cu_4Ti_3, calculated for three different processes: heating, atom exchanges, and Frenkel pair production.

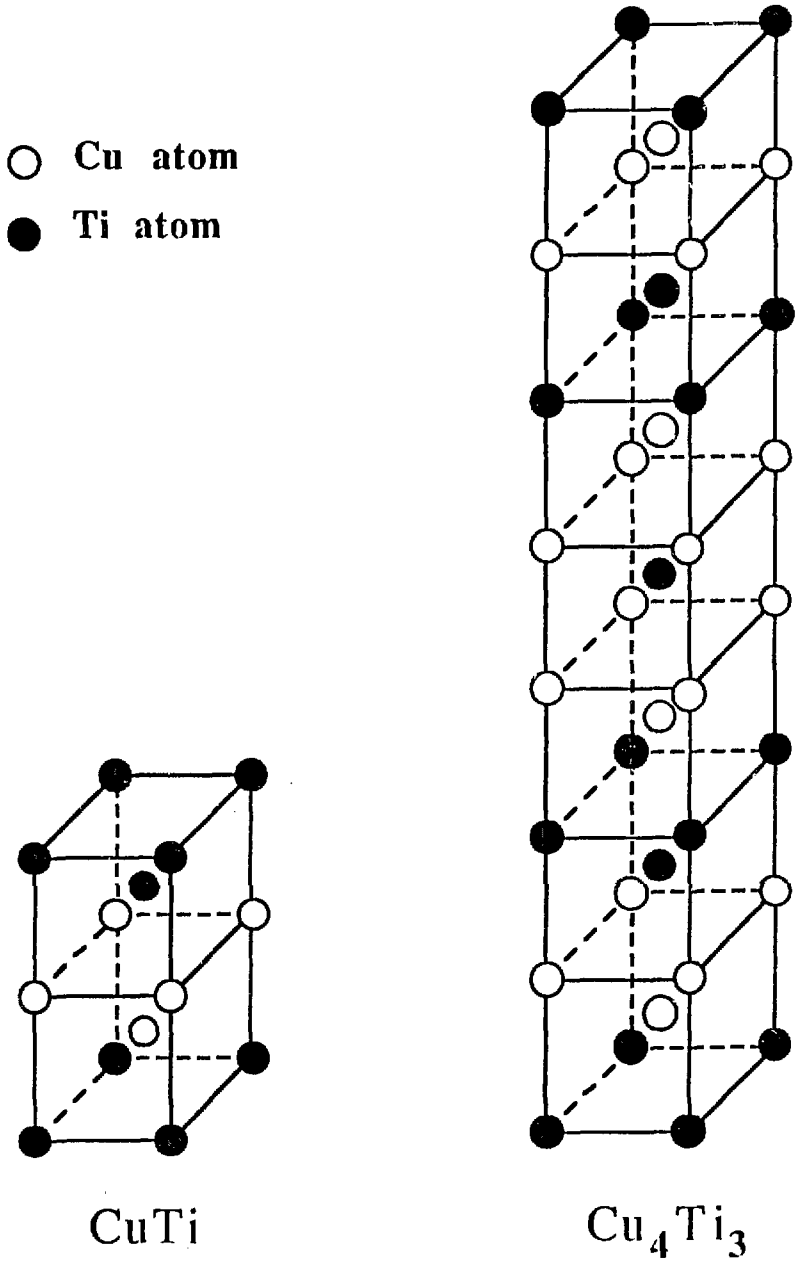

Fig. 1 NiO (AAA structure)

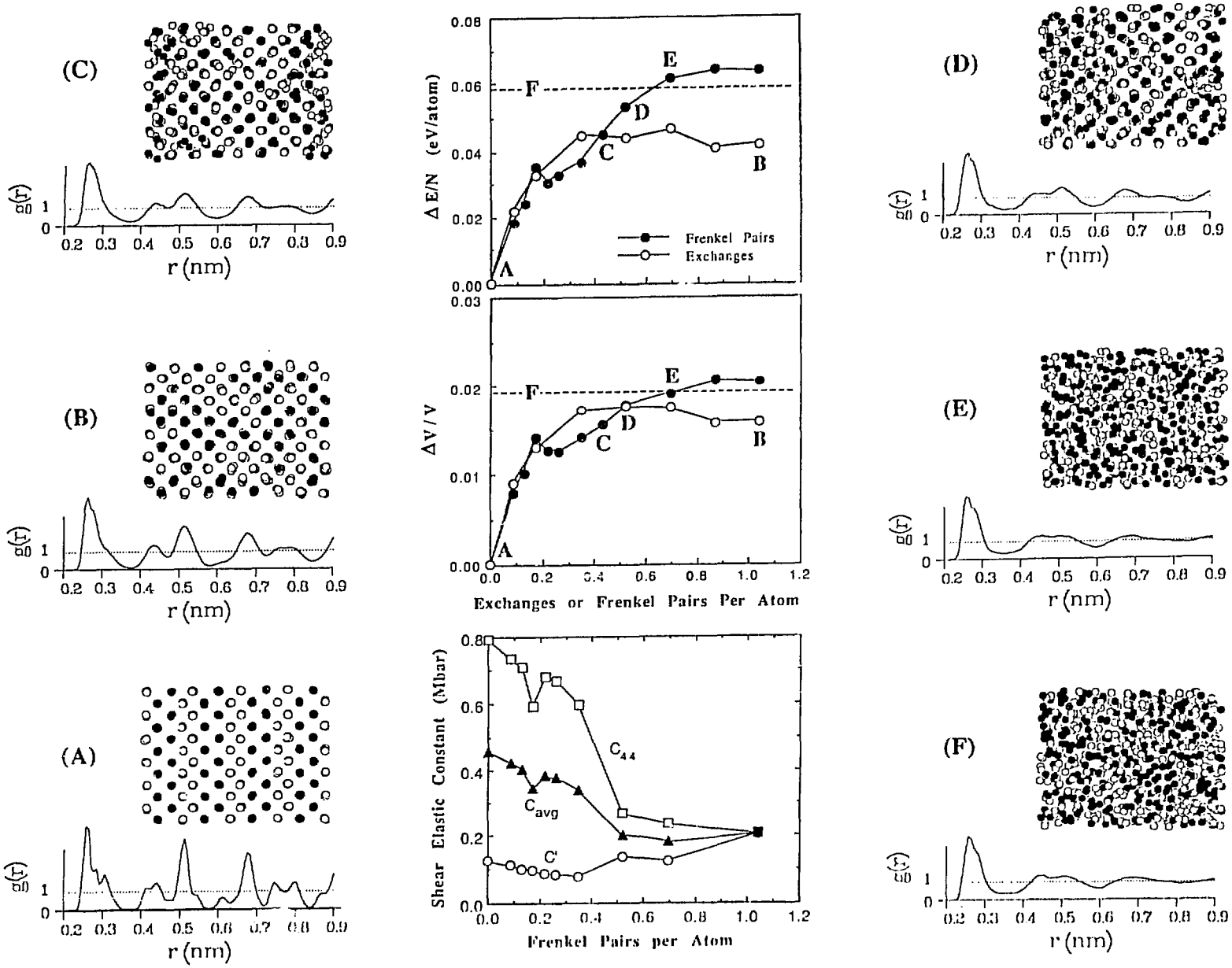

Fig 2 N.Q. Lam et al.

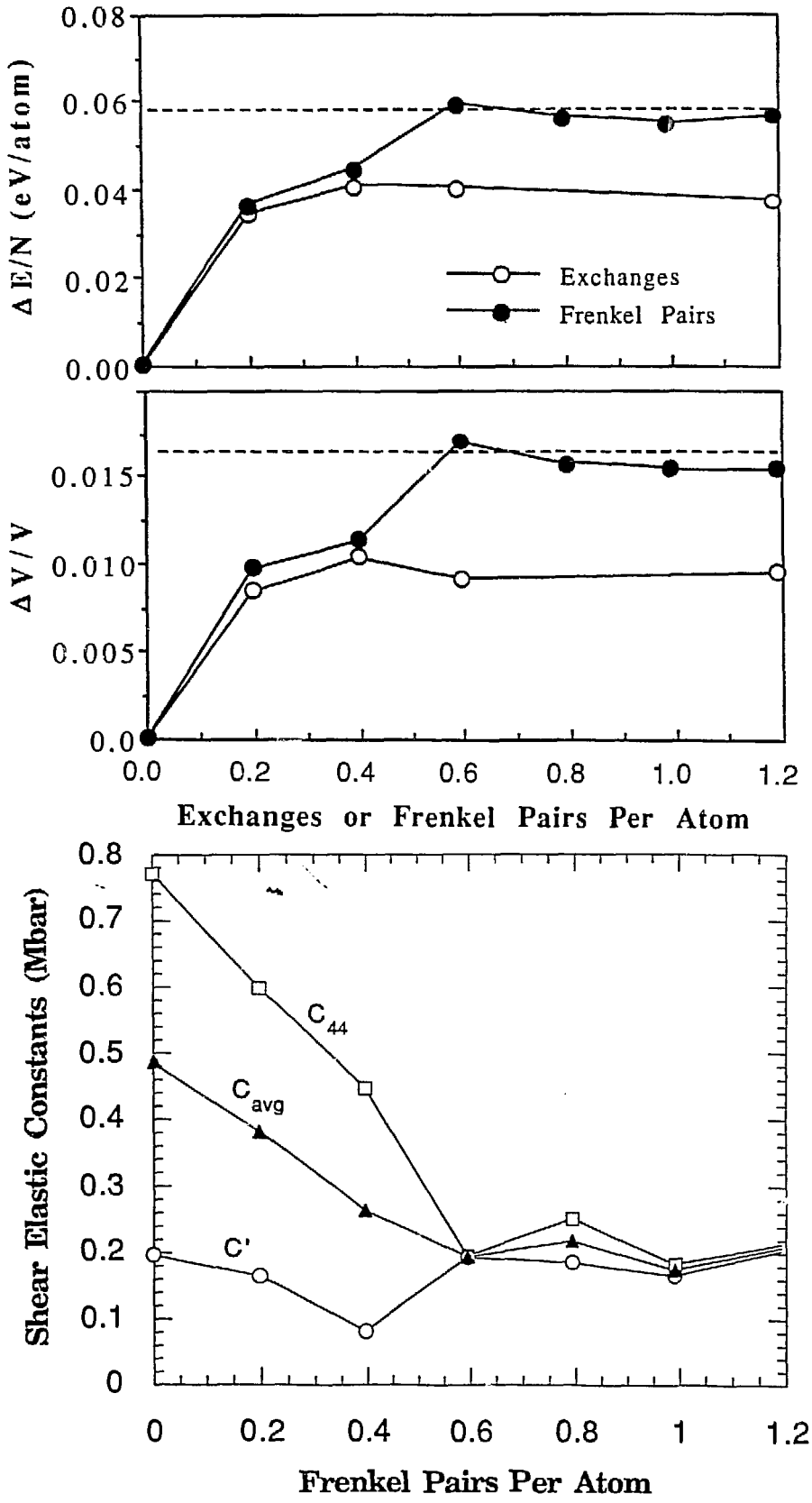
0.08
0.06
0.04
0.02
0.00
ΔE/N (eV/atom)
Exchanges
Frenkel Pairs
0.015
0.010
0.005
0.0
ΔV/V
0.0
0.2
0.4
0.6
0.8
1.0
1.2
Exchanges or Frenkel Pairs Per Atom
0.8
0.7
0.6
0.5
0.4
0.3
0.2
0.1
0
Shear Elastic Constants (Mbar)
C44
Cavg
C'
0
0.2
0.4
0.6
0.8
1
1.2
Frenkel Pairs Per Atom

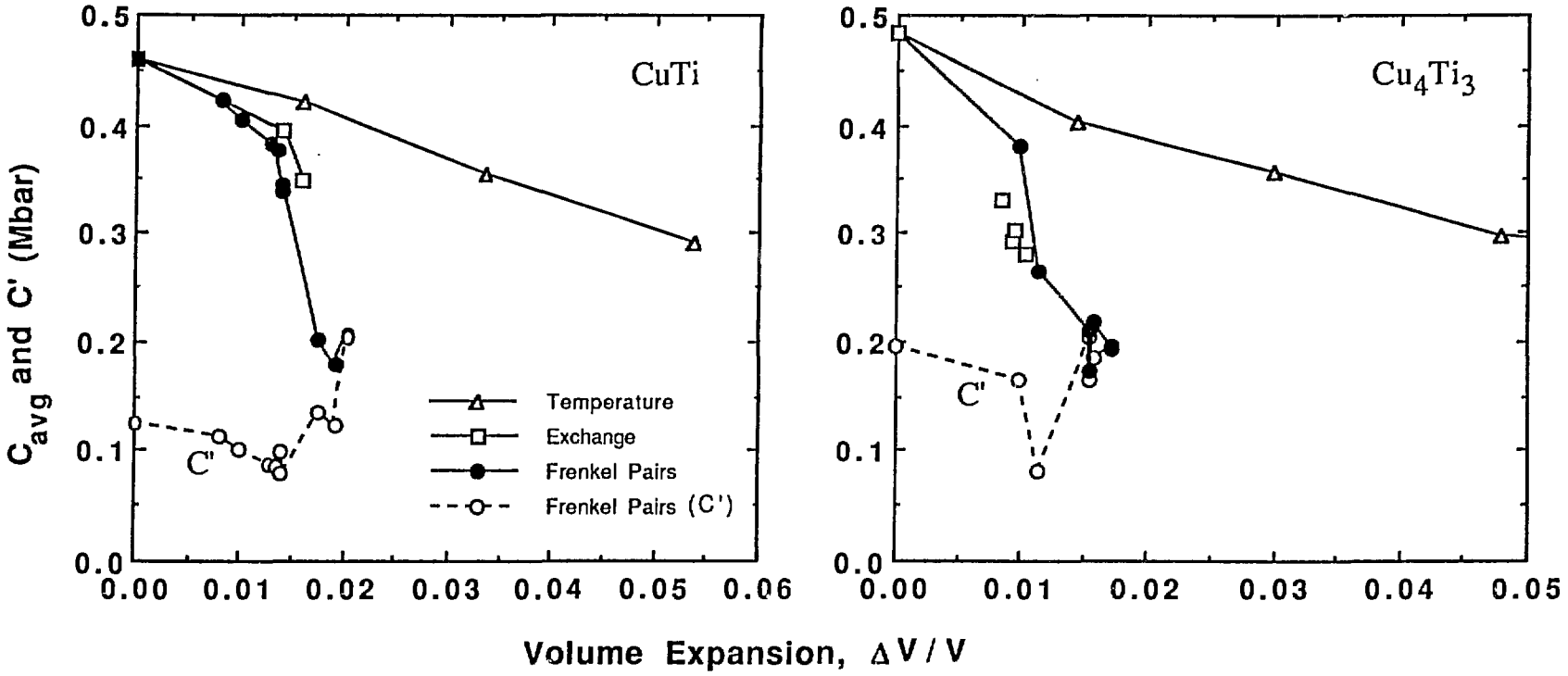

Fig. 4 N.Q. LAM et al.